CHINESE OPTICS LETTERS

Vol. 19, No. 11 | November 2021

All-optical carrier recovery for self-homodyne detection via injection locked Brillouin laser in whispering-gallery-mode microcavity

Boyuan Liu (刘博缘)[1], Yong Geng (耿 勇)[1*], Qiang Zhang (张 强)[1], Xinjie Han (韩鑫洁)[1], Jing Xu (徐 竞)[2], Heng Zhou (周 恒)[1], and Kun Qiu (邱 昆)[1]

[1] School of Information and Communication Engineering, University of Electronic Science and Technology of China, Chengdu 611731, China

[2] Wuhan National Laboratory for Optoelectronics, Huazhong University of Science and Technology, Wuhan 430074, China

*Corresponding author: gengyong@uestc.edu.cn

Received March 22, 2021 | Accepted April 24, 2021 | Posted Online August 24, 2021

We demonstrate comprehensive investigation of the injection locking dynamics of a backscattered Brillouin laser in silica whispering-gallery-mode microcavity. Via injection locking, the Brillouin laser acquires highly correlated phase with the seed laser, enabling ultra-narrow bandwidth, high gain, and coherent optical amplification. Also, for the first time, to the best of our knowledge, the injection locked Brillouin laser is utilized to implement all-optical carrier recovery from coherent optical data signals. We show that by using the injection locked Brillouin laser as a local oscillator for self-homodyne detection, high-quality data receiving can be realized, even without traditional electrical compensations for carrier frequency and phase drifts.

Keywords: optical microcavity; stimulated Brillouin scattering; laser injection locking; self-homodyne detection.
DOI: 10.3788/COL202119.111901

1. Introduction

Coherent data modulation and detection enable high capacity and spectral efficiency optical transmissions by encoding multi-level quadrature information onto both the amplitude and phase of a laser carrier. At the receiver, the arrived coherent data signal is demodulated by mixing itself with a local oscillator (LO)[1,2]. Ideally, the frequency and phase of the LO laser are supposed to be stabilized to the arrived data carrier, so that the down converted intermediate frequency signal has steady temporal waveform, from which the encoded quadrature information can be retrieved with low error rate. However, in today's coherent communication system, the data carrier and LO are usually made of independent lasers, which have weak mutual coherence and thus entail complex digital signal processing (DSP) hardware circuits and software algorithms to calibrate the random frequency and phase walk-off between the carrier and LO[3]. However, DSP-based frequency offset estimation (FOE) and carrier phase estimation (CPE) usually require considerable power consumption[4], which scales up quickly with the increase of data capacity per channel and the number of data channels. So, nowadays, it is becoming more and more important regarding how to regulate the carrier-LO frequency and phase stability in the optical domain instead of referring to electrical compensations.

A potential solution is known as the self-homodyne detection (SHD) technique[5–7]. For an SHD receiver, it all-optically recovers the carrier tone from the transmitted data signal and uses it as the LO for coherent detection[8–12]. As long as the recovered LO inherits the same frequency and phase from the data carrier itself, DSP-aided FOE and CPE can be minimized or even totally dispensed with, thus substantially reducing the complexity and energy consumption of a coherent receiver. To date, all-optical carrier recovery for SHD has been implemented by various approaches; for example, the carrier tone can be extracted from the data signal using passive narrowband filters built by high-finesse optical cavities[8]. Also, it has been demonstrated that carrier recovery can be implemented by using narrowband optical gain provided by laser injection locking[9], stimulated Brillouin scattering (SBS)[10–12], and Kerr parametric amplification[13].

The performance metrics of all-optical carrier recovery include the following parameters. First, the spectral bandwidth for carrier extraction needs to be as small as possible, so that the data component can be located as close as possible to the carrier tone, thus maximizing the spectrum utilization. Second, the optical signal-to-noise ratio (OSNR) of the recovered carrier should be as high as possible (namely, the spectral component of the data signal should be excluded as clear as possible), so that

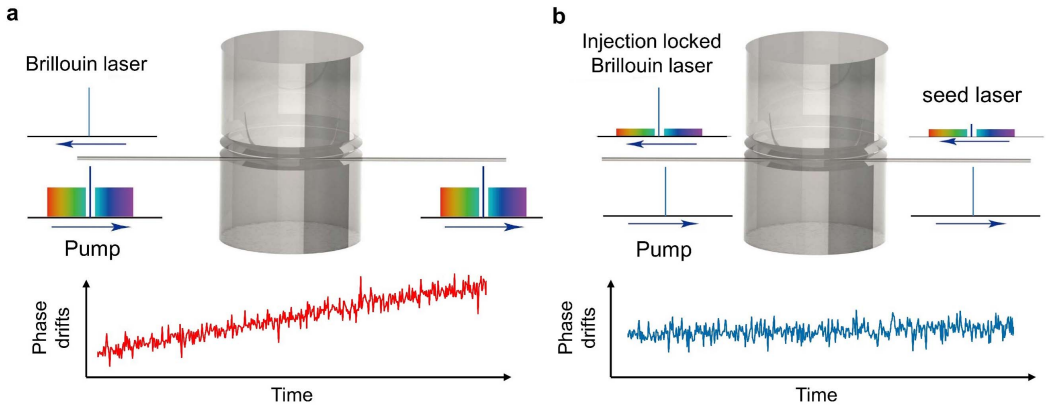

Fig. 1. Comparison of all-optical carrier recovery using (a) free-running and (b) injection locked Brillouin laser in optical microcavity.

residual high-frequency noise attached to the LO tone is avoided. Third, it will be beneficial if the carrier tone can be amplified while being extracted from the data signal. To this extent, carrier recovery methods implemented via nonlinear effects such as SBS[10–12] and parametric amplifications[13] are especially attractive, as these methods can provide substantial amplifications of the picked-up carrier to access high power and high OSNR for the LO tone. Fourth, and most essential, the frequency and phase of the carrier tone should be conserved as being extracted from the data signal, so that SHDs without needing extra electrical processes for FOE and CPE are warranted[2,5].

As demonstrated in our recent work[12], a Brillouin laser generated in high-*Q* silica whispering-gallery mode (WGM) microcavity can be a prominent tool to realize all-optical carrier recovery, as it provides a high gain factor, ultra-narrow gain spectrum, and high carrier OSNR thanks to its backward scattering feature and ease of realization. In particular, when the data carrier tone is tuned into a resonance mode of the microcavity, it will be resonantly enhanced, while the high-frequency data components outside the resonance linewidth are kept small. When reaching the threshold, the data carrier alone will trigger lasing within the gain bandwidth of SBS, which propagates backward with the original input signal and thus can be separated from the data components and used as LO, as shown in Fig. 1(a). However, due to the linewidth compression nature of a Brillouin laser with respect to the pump laser[14–19], in the scenario of carrier recovery[12], the extracted LO tone (i.e., the Brillouin laser itself) is not phase coherent with the original data carrier (i.e., the pump laser), therefore strongly degrading the applicability of the Brillouin laser for all-optical carrier recover and SHD.

More recently, it has been reported that Brillouin lasing dynamics in a silicon opto-mechanics resonator and silica spherical microcavity can be injection-locked by launching a small seed laser within the Brillouin gain spectrum[20,21]. By injection locking the Brillouin laser, the seed laser can be substantially amplified while maintaining its phase coherence. We note that this new physical phenomenon is a perfect solution to overcome the shortcoming of the traditional Brillouin laser for all-optical carrier recovery. In particular, as shown in Fig. 1(b), if we use the data carrier as the seed laser to realize injection locking of a Brillouin laser, it becomes a substantially amplified copy of the carrier tone whose phase coherence is conserved, facilitating SHD data receiving. Nevertheless, the silicon Brillouin laser reported in literature[20] is based on forward Brillouin scattering and thus co-propagates with the pump laser with a quite small Stokes frequency shift of about 6.0 GHz[17], so it was difficult to separate the generated and injection locked Brillouin laser from the pump laser, making it unsuitable for all-optical carrier recovery.

Here, we demonstrate comprehensive investigation of the injection locking dynamics of a backscattered Brillouin laser in a silica WGM microcavity[21]. Also, we demonstrate for the first time, to the best of our knowledge, that by using the injection locked Brillouin laser as the recovered carrier and LO, high-performance SHD data receiving can be achieved even without traditional electrical FOE and CPE.

2. Experiments and Discussions

The experimental setup is shown in Fig. 2(a). We adopt a silica WGM micro-rod cavity as the Brillouin laser platform. The WGM cavity is fabricated by CO_2 laser machining on an ultra-low loss silica rod[22,23]. The diameter of the cavity is about 2.8 mm, corresponding to a free-spectral range (FSR) of about 21.6 GHz. With the optimized CO_2 laser cutting and annealing process, the microcavity can reach a loaded *Q*-factor of above one billion, as revealed by the ringdown measurement shown in Fig. 2(b). Also, during fabrication, we chose a proper thickness and profile for the micro-rod sidewall to obtain a suitable transversal mode density, so that the inter-modal SBS laser with matched Stokes frequency shift (about 11.11 GHz in our experiment) can be readily obtained[19]. To trigger Brillouin lasing, a continuous-wave pump laser with 0.1 kHz fundamental linewidth and 40 mW launched power is coupled into the microcavity via a tapered fiber. The pump laser is finely tuned from higher to lower frequency with a resolution of 100 MHz following the typical thermal triangle of the cavity mode around 1550.014 nm.

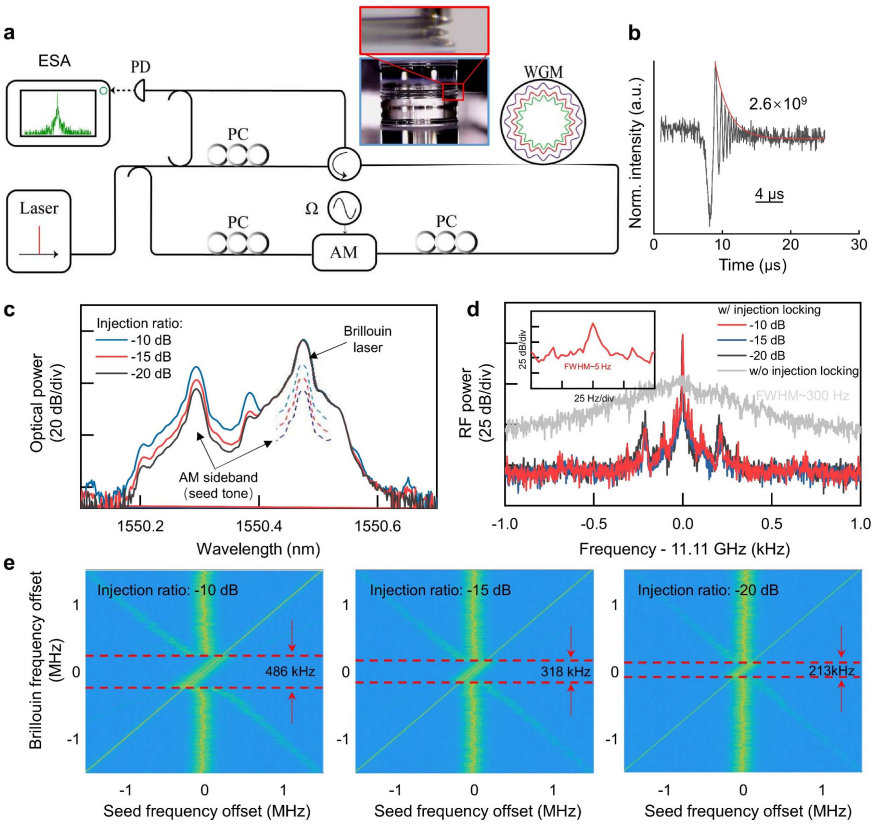

Fig. 2. Demonstration of injection locking of a Brillouin laser in a WGM microcavity. (a) Experimental setup of our study. The inset shows the optical microscopic photo of the silica micro-rod cavity used in our experiment. (b) Ring down measurement of a microcavity mode exhibiting a *Q*-factor of 2.6 billion. (c) Optical spectra of the Brillouin laser and the AM sideband used as the seed laser. (d) Comparison of the beat note between the generated Brillouin laser and the pump laser with or without injection locking. The inset shows the close-up beat note spectrum at −10 dB injection ratio. (e) Injection locking range of Brillouin laser under different injection ratios.

When reaching the threshold, the Brillouin laser in the backward direction can be observed with a power conversion efficiency of about −15.0 dB and at the Stokes frequency shift of about 11.11 GHz with respect to the pump laser, as shown in Fig. 2(c). To test the phase coherence between the Brillouin laser and the pump laser, they are combined in a fiber coupler and sent into a fast photodiode to produce the 11.11 GHz RF beat note, measured using an electrical spectrum analyzer, as shown in Fig. 2(d). At this point, the beat note between Brillouin and pump lasers has a full width half-maximum (FWHM) linewidth of about 0.3 kHz, as shown in Fig. 2(d), indicating weak coherence between them, since the Brillouin laser is supposed to have narrower linewidth (i.e., uncorrelated phase) than the pump laser[12,14,15,24]. Also, it should be clarified that the beat note is also slightly wider than the pump laser linewidth, caused by technique noises such as the thermal frequency drift of cavity resonance and coupling fluctuation between the tapered fiber and micro-rod.

Then, we modulated the pump laser using a Mach–Zehnder modulator (MZM) to generate a 11.11 GHz amplitude modulation (AM) sideband as the seed laser tone and send it into the microcavity from the backward direction (i.e., the same direction as the Brillouin laser, opposite direction to the pump laser). The seed laser power is set to be 10–20 dB lower than the pump laser power (i.e., the injection ratio ranges from −10 to −20 dB), as shown in Fig. 2(c). The modulation frequency derived from a microwave synthesizer is precisely tuned at 2.0 kHz steps, letting the seed laser frequency scan across the Brillouin gain bandwidth. It is observed that once the seed laser is tuned to a proper frequency range, the beat note between the pump and SBS laser shrinks by two orders of magnitude to within 5.0 Hz, consistent with the spectrum linewidth of the 11. 11 GHz RF signal, as shown in Fig. 2(d). Such dynamics is a deterministic signature that the Brillouin laser is injection-locked by the seed laser, which has coherent phase with the pump laser and passes such coherence to the Brillouin laser, therefore producing such narrow beat notes[17]. Moreover, we also measured the injection locking range of the Brillouin laser at different injection ratios, as shown in Fig. 2(d). It is seen that at −10 dB injection ratio the locking range is 486 kHz, while at the −20 dB injection ratio the locking range reduces to 213 kHz.

Next, we explore the injection locked Brillouin laser to facilitate all-optical carrier recovery in the scenario of coherent optical communication. As illustrated in Fig. 3(a), first, an in-phase and quadrature (IQ) modulator is utilized to generate 18.0 Gbaud 16-quadrature amplitude modulation (QAM)

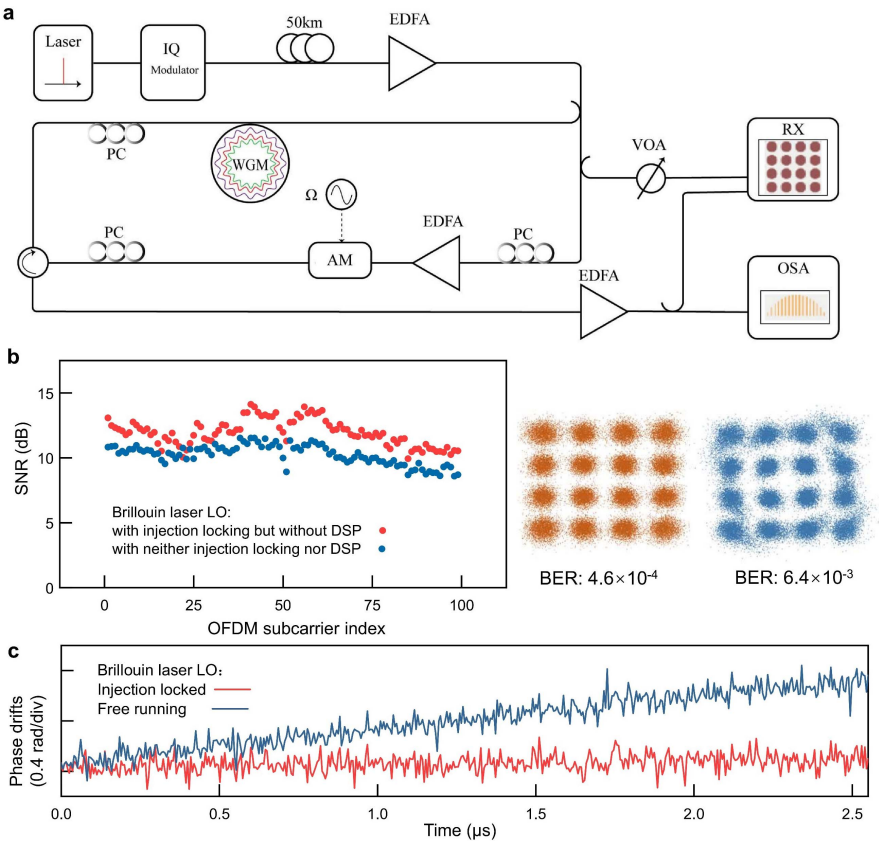

Fig. 3. Demonstration of all-optical recovery and SHD data receiving using injection locked Brillouin laser. (a) Experimental setup. (b) SNR, constellation map, and BER measurement of the received 16-QAM OFDM data signal. (c) Phase drifts between the data signal and LO using injection locked and free-running Brillouin lasers.

optical orthogonal frequency division multiplexing (OFDM) data signal[12,13]. During data modulation, the carrier tone is made 20 dB higher than the data spectrum aside to warrant high OSNR of the recovered carrier, as will be discussed in the following text. The generated 16-QAM OFDM data signal is transmitted over a 50 km single mode fiber to the receiver side. At the receiver, a Brillouin laser is generated within the WGM microcavity, as described in the above paragraph. Then, the carrier tone of the conveyed 16-QAM data signal is used as the seed laser to realize injection locking of the Brillouin laser. The injection ratio is configured to −15 dB by an erbium-doped fiber amplifier (EDFA) that amplifies the arrived data signal. Note, in our experiment, the pump laser and the data signal are derived from the same laser device and frequency separated by 11.11 GHz via AM; therefore, the data carrier automatically lies within the injection range of the Brillouin laser. Practically, the arrived data signal and, particularly, the central carrier tone can be frequency-shifted and directly used as the pump laser for Brillouin laser generation[10,12]. Alternatively, aligning of the seed and Brillouin laser spectra can be done by constantly tuning the Brillouin laser frequency, via changing the pump power or frequency[25,26], to actively track the random frequency wander of the data carrier tone. Moreover, as the carrier tone at the center of the data spectrum is set 20 dB higher than the OFDM subcarrier components, the carrier tone alone injection locks the Brillouin laser, while the data subcarriers merely set a small noise background. After injection locking, the Brillouin laser (namely the recovered data carrier) has an OSNR of about 35.0 dB.

The Brillouin laser is then coupled out from the microcavity and sent into the IQ receiver as the LO for coherent SHD receiving. At the input of the coherent receiver, the data signal power is set to −19 dBm, and the LO power is 10 dBm. Figure 3(b) summarizes the data receiving performance under different configurations. It is seen that when the injection locked Brillouin laser is used as the LO, high-performance SHD receiving can be achieved even when the DSP-based FOE and CPE algorithms are totally dispensed with. Particularly, the SNR is > 10 dB for each of the OFDM subcarriers, and the overall bit error rate (BER) of all subcarriers is as small as 4.6×10^{-4}. The benefit of injection locking is also confirmed by the highly stable carrier phase between the data signal and the Brillouin laser LO, as shown in Fig. 3(c). For this proof-of-concept experiment, the phase drift curves are obtained by directly comparing the 16-QAM symbols demodulated by the receiver, with the original symbols sent from the transmitter[13]. To the contrary, when injection locking is not implemented, the free-running Brillouin laser serving as the LO cannot correctly demodulate

the 16-QAM data without conducting electrical CPE algorithms, due to their uncorrelated phases [also see Fig. 3(c)]. Finally, it should be mentioned that in our experiment we used a low-noise laser with 0.1 kHz fundamental linewidth as the data carrier, which to some extent obscures the strength of an injection locked Brillouin laser as the recovered LO, since even the unlocked Brillouin laser possesses relatively narrow beat notes [0.3 kHz, see Fig. 2(c)] and correspondingly stable phases [see Fig. 3(c)] within the data length (2.5 μs). In practice, when the carrier laser is of larger linewidth, injection locking of the Brillouin laser will become much more beneficial in comparison with the unlocked Brillouin laser[12,27,28].

3. Conclusion

We have demonstrated injection locking of backscattered Brillouin laser in a silica WGM microcavity. It has been observed that the frequency and phase of the seed laser can be faithfully imposed to the Brillouin laser within an injection range of 486 kHz (213 kHz) at the injection ratio of −10 dB (−20 dB). Such new dynamics of Brillouin laser injection locking empowers an ultra-narrow bandwidth, high gain, and coherent optical amplification, which is utilized to realize all-optical carrier recovery for SHD data receiving of high-speed 16-QAM OFDM signals. We have showed that by using the injection locked Brillouin laser as the recovered LO, SHD receiving with high SNR and low BER can be realized even without conducting traditional FOE and CPE algorithms, providing a potential solution to deal with the impending energy crisis that bothers the optical fiber communication industry.

Acknowledgement

This work was supported by the National Key Research and Development Program of China (No. 2019YFB2203103) and the National Natural Science Foundation of China (Nos. 62001086 and 61705033).

References

1. P. J. Winzer, D. T. Neilson, and A. R. Chraplyvy, "Fiber-optic transmission and networking: the previous 20 and the next 20 years," Opt. Express **26**, 24190 (2018).
2. E. Ip, A. P. T. Lau, D. J. F. Barros, and J. M. Kahn, "Coherent detection in optical fiber systems," Opt. Express **16**, 753 (2008).
3. X. Liu, S. Chandrasekhar, and P. J. Winzer, "Digital signal processing techniques enabling multi-Tb/s superchannel transmission: an overview of recent advances in DSP-enabled superchannels," IEEE Signal Process. Mag. **31**, 16 (2014).
4. C. Laperle and M. O'Sullivan, "Advances in high-speed DACs, ADCs, and DSP for optical coherent transceivers," J. Lightwave Technol. **32**, 629 (2014).
5. B. J. Puttnam, R. S. Luis, J. M. Delgado Mendinueta, J. Sakaguchi, W. Klaus, Y. Kamio, M. Nakamura, N. Wada, Y. Awaji, A. Kanno, T. Kawanishi, and T. Miyazaki, "Self-homodyne detection in optical communication systems," Photonics **1**, 110 (2014).
6. B. J. Puttnam, R. Luis, J.-M. Delgado-Mendinueta, J. Sakaguchi, W. Klaus, Y. Awaji, N. Wada, A. Kanno, and T. Kawanishi, "High-capacity self-homodyne PDM-WDM-SDM transmission in a 19-core fiber," Opt. Express **22**, 21185 (2014).
7. M. Mazur, A. Lorences-Riesgo, J. Schroder, P. A. Andrekson, and M. Karlsson, "10 Tb/s PM-64QAM self-homodyne comb-based superchannel transmission with 4% shared pilot tone overhead," J. Lightwave Technol. **36**, 3176 (2018).
8. S. Adhikari, S. L. Jansen, M. Alfiad, B. Inan, A. Lobato, V. A. J. M. Sleiffer, and W. Rosenkranz, "Experimental investigation of self coherent optical OFDM systems using Fabry–Perot filters for carrier extraction," in *36th European Conference and Exhibition on Optical Communication* (2010), p. 1.
9. Z. Liu, J.-Y. Kim, D. J. Richardson, and R. Slavík, "Homodyne OFDM with optical injection locking for carrier recovery," J. Lightwave Technol. **33**, 34 (2015).
10. E. Giacoumidis, A. Choudhary, E. Magi, D. Marpaung, K. Vu, P. Ma, D. Y. Choi, S. Madden, B. Corcoran, M. Pelusi, and B. J. Eggleton, "Chip-based Brillouin processing for carrier recovery in self-coherent optical communications," Optica **5**, 1191 (2018).
11. M. Pelusi, A. Choudhary, T. Inoue, D. Marpaung, B. J. Eggleton, K. S. Trapala, H. N. Tan, and S. Namiki, "Frequency comb noise suppressor by a Brillouin comb amplifier for phase sensitive communications," Opt. Express **25**, 17847 (2017).
12. Q. Wen, J. Qin, Y. Geng, G. Deng, Q. Zhou, H. Zhou, and K. Qiu, "Stimulated Brillouin laser-based carrier recovery in a high-*Q* microcavity for coherent detection," Opt. Lett. **45**, 3848 (2020).
13. Y. Geng, W. Cui, Q. Wen, B. Wang, Q. Zhou, B. Wu, and H. Zhou, "Microcavity-based narrowband parametric amplifier for carrier recovery in optical coherent self-homodyne detection," Opt. Lett. **44**, 3490 (2019).
14. A. Debut, S. Randoux, and J. Zemmouri, "Linewidth narrowing in Brillouin lasers: theoretical analysis," Phys. Rev. A **62**, 023803 (2000).
15. W. Loh, S. B. Papp, and S. A. Diddams, "Noise and dynamics of stimulated-Brillouin-scattering microresonator lasers," Phys. Rev. A **91**, 053843 (2015).
16. S. Gundavarapu, G. M. Brodnik, M. Puckett, T. Huffman, D. Bose, R. Behunin, J. Wu, T. Qiu, C. Pinho, N. Chauhan, J. Nohava, P. T. Rakich, K. D. Nelson, M. Salit, and D. J. Blumenthal, "Sub-hertz fundamental linewidth photonic integrated Brillouin laser," Nat. Photon. **13**, 60 (2019).
17. N. T. Otterstrom, R. O. Behunin, E. A. Kittlaus, Z. Wang, and P. T. Rakich, "A silicon Brillouin laser," Science **360**, 1113 (2018).
18. L. Sheng, D. Ba, and Z. Lü, "Weak laser pulse signal amplification based on a fiber Brillouin amplifier," Chin. Opt. Lett. **16**, 111901 (2018).
19. Y. Bai, M. Zhang, Q. Shi, S. Ding, Y. Qin, Z. Xie, X. Jiang, and M. Xiao, "Brillouin–Kerr soliton frequency combs in an optical microresonator," Phys. Rev. Lett. **126**, 063901 (2021).
20. N. T. Otterstrom, S. Gertler, Y. Zhou, E. A. Kittlaus, R. O. Behunin, M. Gehl, A. L. Starbuck, C. M. Dallo, A. T. Pomerene, D. C. Trotter, A. L. Lentine, and P. T. Rakich, "Backscatter-immune injection-locked Brillouin laser in silicon," Phys. Rev. A **14**, 044042 (2020).
21. F. Zhang, Y. Feng, X. Chen, L. Ge, and W. Wan, "Synthetic anti-PT symmetry in a single microcavity," Phys. Rev. Lett. **124**, 053901 (2020).
22. P. Del'Haye, S. A. Diddams, and S. B. Papp, "Laser-machined ultra-high-*Q* microrod resonators for nonlinear optics," Appl. Phys. Lett. **102**, 221119 (2013).
23. Q. Wen, W. Cui, Y. Geng, H. Zhou, and K. Qiu, "Precise control of micro-rod resonator free spectral range via iterative laser annealing," Chin. Opt. Lett. **19**, 071903 (2021).
24. D. A. Korobko, I. O. Zolotovskii, V. V. Svetukhin, A. V. Zhukov, A. N. Fomin, C. V. Borisova, and A. A. Fotiadi, "Detuning effects in Brillouin ring microresonator laser," Opt. Express **28**, 4962 (2020).
25. Z. Liu and R. Slavík, "Optical injection locking: from principle to applications," J. Lightwave Technol. **38**, 43 (2020).
26. W. Loh, A. A. S. Green, F. N. Baynes, D. C. Cole, F. J. Quinlan, H. Lee, K. J. Vahala, S. B. Papp, and S. A. Diddams, "Dual-microcavity narrow-linewidth Brillouin laser," Optica **2**, 225 (2015).
27. X. Yi, W. Shieh, and Y. Tang, "Phase estimation for coherent optical OFDM," IEEE Photon. Technol. Lett. **19**, 919 (2007).
28. X. Fang and F. Zhang, "Phase noise estimation and suppression for PDM CO-OFDM/OQAM systems," J. Lightwave Technol. **35**, 1837 (2017).